Eur. Phys. J. Special Topics **223**, 2483–2491 (2014)

DOI: 10.1140/epjst/e2014-02213-0

THE EUROPEAN PHYSICAL JOURNAL SPECIAL TOPICS

Regular Article

Basin stability of the Kuramoto-like model in small networks

Peng Ji[1,2,a] and Jürgen Kurths[1,2,3]

[1] Potsdam Institute for Climate Impact Research (PIK), 14473 Potsdam, Germany
[2] Department of Physics, Humboldt University, 12489 Berlin, Germany
[3] Institute for Complex Systems and Mathematical Biology, University of Aberdeen, Aberdeen AB24 3UE, UK

Received 15 January 2014 / Received in final form 12 May 2014
Published online 24 June 2014

Abstract. Power system stability is quantified as the ability to regain an equilibrium state after being subjected to perturbations. We start by investigating the global basin stability of a single machine bus-bar system and then extend it to two and four oscillators. We calculate the basin stability of the stable fixed point over the whole parameter space, in which different parameter combinations give rise to a stable fixed point and/or a stable limit cycle depending crucially on initial conditions. A governing equation for the limit cycle of the one-machine infinite bus system is derived analytically and these results are found to be in good agreement with numerical simulations.

1 Introduction

The Kuramoto-like model [1–8] has been established as a standard reduced model describing the emergence of collective phenomenon, which are of great interest in various physical systems, especially in power systems [4–6]. Much effort so far has been devoted to investigating the synchronization of power systems. For example, the stability of decentralized power grids against dynamical perturbations and topological failures were investigated in [4], and Dörfler et al. [6] stated elegantly the synchronized condition in terms of complex network topology and parameters.

Linear stability analysis has been applied to characterize local stability in terms of Lyapunov exponents [9]. As modern power system components are often nonlinear, their stability depends on both initial conditions and the amplitude of disturbance [10]. Based on the basin of attraction, Menck et al. [11,12] proposed basin stability, which is non-local and nonlinear and could also be applied to high-dimensional dynamical systems to assess how stable a state is. This stability is quantified as the probability to regain an equilibrium point after being subjected to an even large disturbance [10].

This paper is organized as follows. In Sect. 2, we attempt to explain the basic power grid dynamics using the classical model of a one-machine infinite bus system. We investigate the parameter space of the one-machine infinite bus system using basin

[a] e-mail: pengji@pik-potsdam.de

stability. A stable fixed point and a stable limit cycle coexist in the bistable area. The governing equation of the stable limit cycle is derived analytically, and the analytical results are found to be in good agreement with numerical simulations. The coexistence could also be found in a four-node topology using basin stability. Thus basin stability is used to characterize the parameter space not only in the one-machine infinite bus system but also in a two-node and a four-node topology as shown in Sects. 3 and 4 respectively. In the final section, we summarize our results.

2 Dynamics of the one-machine infinite bus system

2.1 Model

In order to understand the underlying dynamics of the power system, we present a mathematical derivation of the model of the one-machine infinite bus system, which describes one machine (generator or consumer) connected to an infinite busbar via a lossless transmission line [4,10,13,14] The state of the machine is described by its phase angle $\phi(t) = \Omega t + \theta(t)$ and the angular velocity $\dot{\phi}(t)$, where Ω is the average angular speed of the machine and $\theta(t)$ is the phase difference with respect to a synchronously rotating reference frame.

The real power balance equation is represented by

$$P_{source} = P_{dissipated} + P_{kinetic} + P_{transmited}, \tag{1}$$

i.e. the source energy P_{source} must be equal to the sum of dissipated, kinetic and transmitted energies.

The dissipated energy is proportional to the square of the angular velocity:

$$P_{dissipated} = K_D(\dot{\phi})^2, \tag{2}$$

where K_D is the fraction coefficient.

The accumulated kinetic energy is given by

$$P_{kinetic} = \frac{1}{2} I \frac{d}{dt}(\dot{\phi})^2, \tag{3}$$

where I is the moment of inertia.

The energy flow between the machine and the infinite busbar is proportional to the maximal energy transfer capacity P^{MAX} and the sine of the phase difference between the phase θ of the single machine and the phase θ_I of the infinite busbar. The infinite busbar is assumed to be an ideal source of constant voltage and frequency, neither of them is influenced by the action of the machine [10]. Thus, for the sake of convenience, the phase disturbance θ_I of the infinite busbar could be assumed to be 0. So the transmitted power follows

$$P_{transmitted} = P^{MAX} \sin(\theta). \tag{4}$$

Substituting equations (2-4) into equation (1), one obtains

$$P_{source} = I\ddot{\theta}\dot{\phi} + K_D(\dot{\phi})^2 + P^{MAX} \sin(\theta). \tag{5}$$

In the limit of a small perturbation of the synchronous frequency $\dot{\theta} \ll \Omega$, $I\ddot{\theta}$ and $K_D\dot{\theta}^2$ can be neglected compared to $I\ddot{\theta}\Omega$ and $K_D\Omega^2$ respectively. Defining $P \equiv (P_{source} - K_D\Omega^2)/(I\Omega)$, $\alpha \equiv 2K_D/I$ and $K \equiv P^{MAX}/(I\Omega)$, this equation becomes

$$\ddot{\theta} = -\alpha\dot{\theta} + P - K \sin(\theta), \tag{6}$$

which is the governing equation of the dynamics of the one-machine infinite bus system.

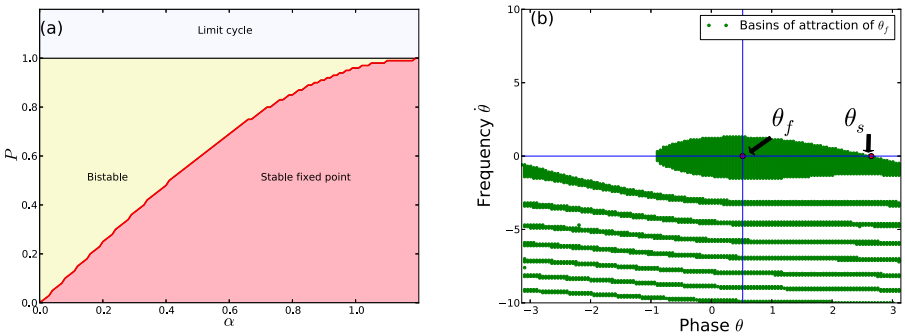

Fig. 1. Parameter space and state space of the one-machine infinite bus system. In the left panel (a), red indicates the area of stable fixed point. In the yellow area, the oscillator either converges to stable fixed point or rotates periodically depending crucially on initial values of θ and $\dot{\theta}$. White area indicates the existence of stable limit cycle. (b) Basin of attraction of the stable fixed point θ_f is indicated in the green area with $\alpha = 0.1$, $P = 0.5$ and $K = 1$. The stable fixed point and saddle are also plotted in red. The saddle is at the right side of the stable fixed point.

2.2 Basin stability

Defining the relative size of the volume of basin of attraction as basin stability $S \in [0, 1]$, a new non-local and nonlinear measure was recently proposed to quantify how stable the synchronous sate is against even large perturbations [11]. To estimate the basin stability of a stable fixed point in case of single machine infinite bus system, we randomly select 25000 initial values of $(\theta, \dot{\theta})$ from $[-\pi, \pi] \times [-10, 10]$, integrate the system long enough and then count the percentage of initial values reaching a stable fixed point.

According to the stability diagram of the one-machine infinite bus system as shown in Fig. 1a [15–18], a stable fixed point and a stable limit cycle coexist in the bistable area (colored in yellow). Whether the system will evolve to the fixed point or to the limit cycle depends crucially on the initial conditions. When parameter values are located in the limit cycle area (resp. stable fixed point area) S is 0 (resp. 1). Shown in Fig. 1b is the phase space of the one-machine infinite bus system for a set of parameter values corresponding to the bistable area in Fig. 1a. The system has one stable fixed point $\theta_f = \arcsin(P/K)$ for $0 < P < K$, and one saddle $\theta_s = \pi - \theta_f$. The basin of attraction of the stable fixed point θ_f is colored green and that of the stable limit cycle is colored white. The saddle is located on the right side of the stable fixed point at the intersection between the basin of attraction of θ_f and $\dot{\theta} = 0$ line.

In Fig. 2, we project the basin stability S over the parameter space of the one-machine infinite bus system for $K = 1$. As can be observed from Fig. 2, basin stability increases with α in the bistable area, and then jumps to unity when α crosses the homoclinic bifurcation line $\alpha = \frac{P\pi}{4\sqrt{K}}$ [15]. It is also evident that one can use basin stability to locate the homoclinic bifurcation line as the locus of the points where basin stability S becomes unity for the first time when α is incremented gradually from 0 to 1.

2.3 Limit cycle

The one-machine infinite bus system is multistable when α is within the range $[0, \frac{P\pi}{4\sqrt{K}}]$ for $P < K$. In Fig. 1b, if we integrate the system long enough with initial parameter

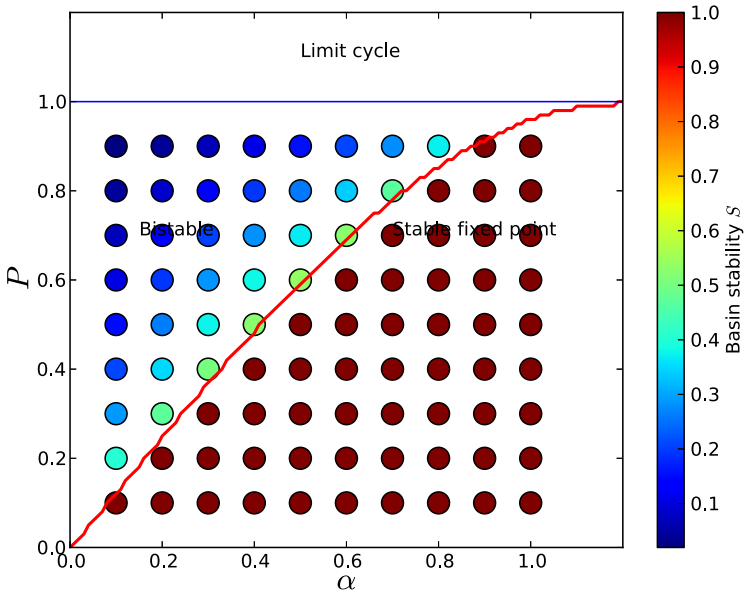

Fig. 2. Basin stability over parameter space of the one-machine infinite bus system. The different areas same as shown the Fig. 1a are separated by the two lines: $P/K = 1$ and the homoclinic bifurcation line. When $\alpha \to 0$, the bifurcation line is tangent to the line $\alpha = P\pi/(4\sqrt{K})$. For fixed coupling strength $K = 1$, basin stability S is calculated over the parameter space by varying the value of α and P from 0 to 1 separately.

values from the white area, the system will rotate periodically. In order to deepen the understanding of the dependency of $\dot{\theta}$ on θ, we seek to describe the phase portrait on the θ-$\dot{\theta}$ plane. Referring to the simulation curve as shown in Fig. 3, $\sum_{t=0}^{T} \sin(\theta(t)) = 0$ and $\sum_{t=0}^{T} \sin(\dot{\theta}(t)) = 0$, where t denotes the time and T one period. Therefore, from Eq. (6), we get the average value of frequency $\langle\dot{\theta}\rangle \simeq P/\alpha$. The frequency $\dot{\theta}$ as a function of the phase θ is assumed as following:

$$\dot{\theta} = A\cos(\theta) + P/\alpha, \tag{7}$$

where A is the amplitude. Substituting equation (7) into Eq. (6) and setting $\cos(\theta) = 0$, one finds

$$A = K\alpha/P, \tag{8}$$

which means that the amplitude of the oscillation is proportional to K and α. With increasing coupling strength K or dissipation coefficient α, the state of the system changes from the stable limit cycle to the stable fixed point as shown in Fig. 1b. If the generated or consumed power P is increased, the amplitude decreases and it becomes more and more difficult to converge to the fixed point.

Selecting a random set of initial values for θ and $\dot{\theta}$ from the white area of Fig. 1b, and integrating the system for a long time, we obtain the stable limit cycle as plotted in Fig. 3. The analytic curve from Eq. (7) is plotted in red. The analytic and simulation curves match very well.

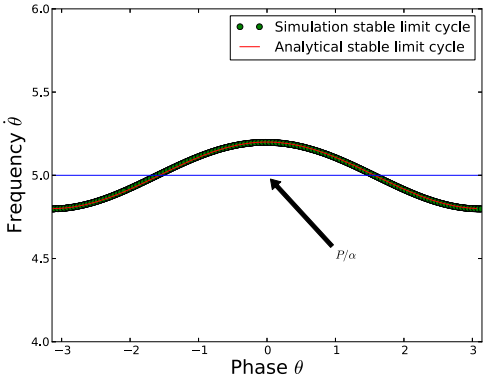

Fig. 3. Stable limit cycle is shown. The green curve is plotted from simulation for $\alpha = 0.1$, $P = 0.5$ and $K = 1$. The system oscillates around P/α. The red curve is obtained from Eq. (7).

2.4 Maximum Lyapunov exponent

Eigenvalues λ of the Jacobian matrix J of the one-machine infinite bus system at $(\theta, \dot{\theta})$ are given by the characteristic equation $det(A - \lambda I) = 0$, that is:

$$\begin{vmatrix} -\lambda & 1 \\ -K\cos(\theta) & -\alpha - \lambda \end{vmatrix} = 0.$$

Solving the determinant we obtain

$$\lambda_{1,2} = \frac{-\alpha \pm \sqrt{\alpha^2 - 4K\cos\theta}}{2}. \tag{9}$$

The maximum Lyapunov exponent of the stable fixed point θ_f is equal to $Re\lambda$ [11]. For the parameter values corresponding to Fig. 1b, if θ converges to the stable fixed point θ_f, $\cos(\theta) \simeq \cos(\theta_f) = 0.86$ and the maximum Lyapunov exponent should be close to $-\alpha/2 = -0.05$. Shown in Fig. 4 is the maximum Lyapunov exponent of the one-machine infinite bus system with the same parameter values as used in Fig. 1b to compare the two methods of calculating the basin of attraction of the stable fixed point. The points with the maximum Lyapunov exponent close to -0.05 are shown in blue color. The area of blue points also shows the state space of the one-machine infinite bus system.

3 Dynamics of two oscillators

What happens if the network is a set of two or more nodes? Consider first two oscillators, out of which one is a generator with $P_g = +P$ and one consumer with $P_c = -P$, the dynamics is governed by

$$\ddot{\theta}_g = -\alpha\dot{\theta}_g + P + K\sin(\theta_c - \theta_g), \tag{10}$$

$$\ddot{\theta}_c = -\alpha\dot{\theta}_c - P + K\sin(\theta_g - \theta_c). \tag{11}$$

The phase difference $\delta\theta = \theta_g - \theta_c$ satisfies

$$\delta\ddot{\theta} = -\alpha\delta\dot{\theta} + 2P + 2K\sin(-\delta\theta), \tag{12}$$

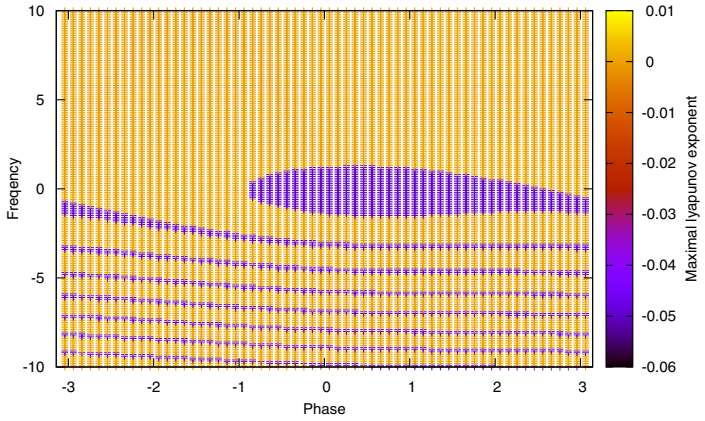

Fig. 4. The maximum Lyapunov exponent of the one-machine infinite bus system for $\alpha = 0.1$, $P = 0.5$ and $K = 1$. If the maximum Lyapunov exponent is smaller than 0, the oscillator converges to the stable fixed point. We can also use the maximum Lyapunov exponent to reproduce the basin of attraction of the stable fixed point.

which is the same as the equation of motion of the one-machine infinite bus system. Following the same process as in Sect. 2, we investigate the dynamics of the two oscillators. For $P > K$, the oscillators converge to one stable limit cycle which oscillates around P/α. For $\frac{4\alpha\sqrt{K}}{\pi} < P < K$, there could be one stable limit cycle and one stable fixed point at

$$\delta\theta = \arcsin(P/K), \tag{13}$$

which depends on initial conditions of $\delta\theta$ and $\delta\dot{\theta}$. Figure 1 illustrates the coexistence of the stable limit cycle and the stable fixed point. Also basin stability S decreases with increasing K from $\frac{4\alpha\sqrt{K}}{\pi}$ to K for fixed α and K. For $K < \frac{4\alpha\sqrt{K}}{\pi}$, only one stable fixed point exists with basin stability $S = 1$.

4 Dynamics of a medium-dimensional dynamical system

4.1 Basin stability with 4 oscillators

In the Sects. 2 and 3, we have shown the coexistence of a stable limit cycle and a stable fixed point in a one-machine infinite bus system and in the two-oscillators topology respectively. Further, basin stability has been used to quantify how stable the fixed point is. What happens when the number of the nodes is increased by 2? Here we focus on the nonlinear stability of four-node topology ranging from a basic ring network with two generators separated by two consumers of Fig. 5a to the network of globally-coupled phase oscillators of Fig. 5d.

The power grid model takes the following form in the simplest case:

$$\ddot{\theta}_i = -\alpha\dot{\theta}_i + P_i + K\sum_{j=1}^{N} A_{ij}\sin(\theta_j - \theta_i), \tag{14}$$

where $N = 4$ and A_{ij} is an element of the network's adjacency matrix A. When oscillators i and j are connected, $A_{ij} = 1$ and $A_{ij} = 0$ otherwise. For the sake of simplicity, we assume that the damping coefficient α is the same for all oscillators.

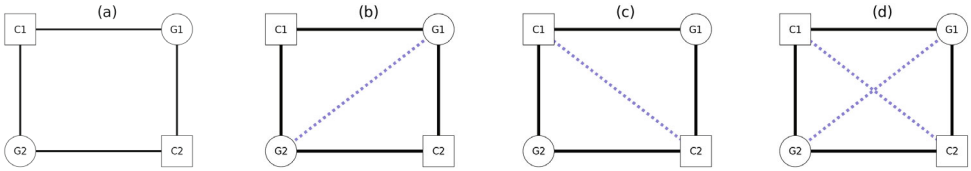

Fig. 5. Connection of 2 generators ($G1$ and $G2$) and 2 consumers ($C1$ and $C2$). Squares denote consumers and circles represent generators. (a) Two generators fully connect to 2 consumers, but the two generators or the two consumers are not connected directly. In configuration (b) (resp. (c)), the two generators (resp. consumers) are also connected with one additional dashed blue diagonal line. (d) Both generators and consumers are fully connected with two additional dashed diagonal lines.

All transmission lines have also been assumed to have identical capacity, and therefore the coupling constant K is the same. The most important feature of a power system is that huge amounts of electricity cannot easily and conveniently be stored [10], which means at any instant of time the net energy consumption has to be met by generation $\sum_i P_i = 0$.

In order to compare the parameter space of a medium-dimensional dynamical system with that of the one-machine infinite bus system, we vary the values of α and P for fixed coupling strength $K = 1$. In Fig. 6, we show basin stability over the parameter space of α and P for the networks combining two generators with $P_{G1} = P_{G2} = P$ and two consumers with $P_{C1} = P_{C2} = -P$ as shown in Fig. 5.

Instead of perturbing only one oscillator [11], in this paper, we perturb all oscillators and then calculate basin stability. In order to assess basin stability, we randomly select for each pair of α and p initial values of $(\theta,\dot{\theta})$ from $[-\pi, \pi] \times [-15, 15]$, integrate the system long enough and then find the percentage of initial values reaching the synchronized state. For every pair of α varying from 0 to 2 with 0.05 interval and P varying from 0 to 2 with the same gap, we repeat the same process to calculate the basin stability and then sketch the parameter space as shown in Fig. 6. This way we find that there are three different regions namely a stable limit cycle, bistability and a stable fixed point. Comparing the parameter space of Fig. 6a and d, we see that the volume of the bistable area decreases as the network becomes more connected.

4.2 Finite-time maximum transverse Lyapunov exponent

In nonlinear dynamics, the convergence/divergence properties of nearby trajectories are quantified by the positive/negative maximum Lyapunov exponent [9]. A stable limit cycle has a zero maximum Lyapunov exponent: it neither grows nor decays in time [9].

To investigate the linear stability, we analyze properties of trajectories converging to the fixed point by calculating the finite-time maximum transverse Lyapunov exponent for $P = 1$, $K = 1$ and increasing α from 0. Next, we randomly draw initial values of θ and $\dot{\theta}$ close to equilibrium points, and integrate the system for a long time. If the oscillators are synchronized, for example at time t, then we calculate the finite-time maximum transverse Lyapunov exponent from t to $t+T$. In the synchronization region, the maximum Lyapunov exponent should be negative. In simulations, we set $T = 10^4$ and compare the rate of convergence for different α.

In Fig. 7, high convergence ratios are corresponding to high dissipating values α. Also there is a constant in the value of maximum Lyapunov exponent with increasing α. Comparing basin stability as shown in Fig. 6 and linear stability as shown in Fig. 7,

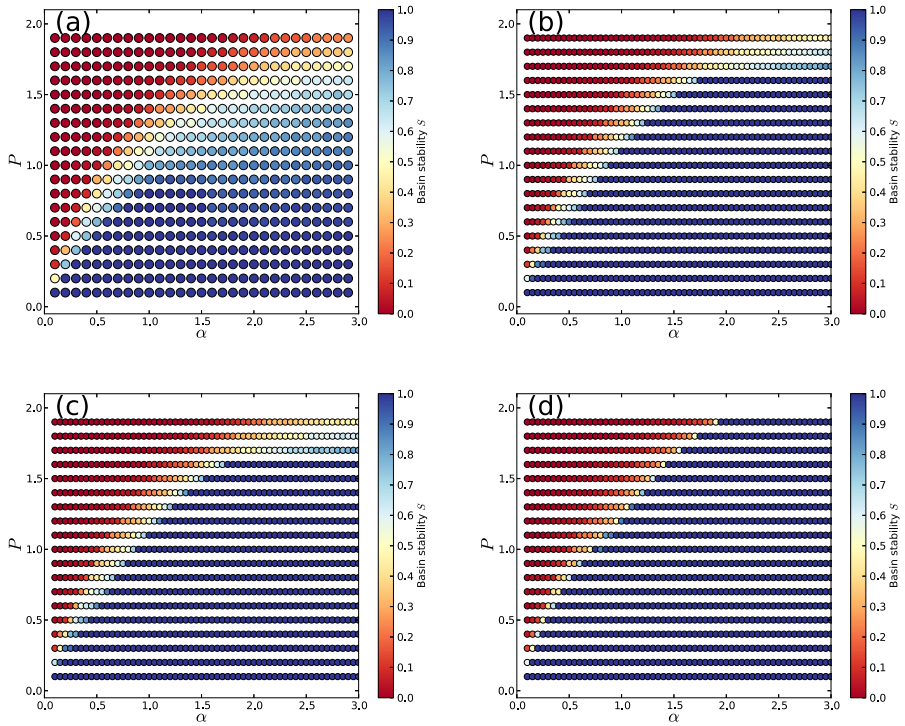

Fig. 6. The panels show basin stability over the parameter space of α and P for $K = 1$ for the networks corresponding to Fig. 5. Comparing the parameter space of (a) and (d), we can see that the volume of the bistable area decreases as the network becomes more connected.

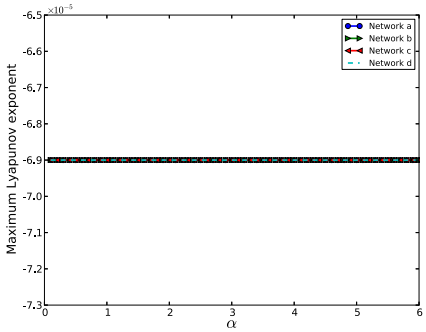

Fig. 7. Finite-time maximum transverse Lyapunov exponent in the networks for Fig. 5. Here $K = 1$ and $P = 1$.

we can get that linear stability is not suitable to evaluate the stability against large perturbations.

5 Conclusions

Parameter values and the size of a disturbance are two crucial factors to determine the stability of a nonlinear power system. Motivated by the question of how stable a state is, basin stability was proposed based on the volume of the basin of attraction.

In this paper, we have evaluated the basin stability for a one-machine infinite bus system and a four-node network. Basin stability has been projected over the parameter space not only for the 2 dimensional system but also for medium dimensional dynamical system. We analytically derived the governing equation of the limit cycle for the one machine infinite bus system and analytical and numerical results match very well. It is instructive to characterize the state space and parameter space in terms by means of Lyapunov exponent. This study illustrates a new way of investigating the stability even for high dimensional systems.

P. Ji is funded by China Scholarschip Council (CSC) scholarship. J. Kurths would like to acknowledge IRTG 1740 (DFG and FAPESP) for the sponsorship provided.

References

1. Y. Kuramoto, H. Arakai, *Chemical oscillations, waves and turbulence* (1984)
2. J.A. Acebrón, L.L. Bonilla, C.J.P. Vicente, F. Ritort, R. Spigler, Rev. Mod. Phys. **77**(1), 137 (2005)
3. A. Arenas, A. Díaz-Guilera, J. Kurths, Y. Moreno, C. Zhou, Phys. Reports **469**(3), 93 (2008)
4. M. Rohden, A. Sorge, M. Timme, D. Witthaut, Phys. Rev. Lett. **109**, 064101 (2012)
5. G. Filatrella, A.H. Nielsen, N.F. Pedersen, Eur. Phys. J. B-Cond. Matter Complex Syst. **61**(4), 485 (2008)
6. F. Dörfler, M. Chertkov, F. Bullo, Proc. Nat. Acad. Sci. **110**(6), 2005 (2013)
7. T.K.D. Peron, F.A. Rodrigues, J. Kurths, Phys. Rev. E **87**, 032807 (2013)
8. A. Pluchino, S. Boccaletti, V. Latora, A. Rapisarda, Physica A: Statistical Mechanics and its Applications **372**(2), 316 (2006)
9. A. Pikovsky, M. Rosenblum, J. Kurths, *Synchronization: a universal concept in nonlinear sciences*, Vol. 12 (Cambridge University Press, 2003)
10. J. Machowski, J. Bialek, J. Bumby, *Power system dynamics: stability and control* (John Wiley & Sons, 2011)
11. P. Menck, J. Heitzig, N. Marwan, J. Kurths, Nat. Phys. **9**, 89 (2013)
12. P. Menck, J. Heitzig, J. Kurths, H.J. Schellnhuber, Nat Commun (in press) (2014)
13. G. Filatrella, A.H. Nielsen, N.F. Pedersen, Eur. Phys. J. B **61**(4), 485 (2008)
14. D. Witthaut, M. Timme, New J. Phys. **14**(8), 083036 (2012)
15. S.H. Strogatz, *Nonlinear Dynamics and Chaos. With Applications to Physics, Chemistry and Engineering* (Reading, PA: Addison-Wesley, 1994)
16. P. Ji, T.K.D. Peron, P.J. Menck, F.A. Rodrigues, J. Kurths, Phys. Rev. Lett. **110**, 218701 (2013)
17. P. Ji, T.K.D. Peron, F.A. Rodrigues, J. Kurths, Scientific Reports **4** (2014)
18. M. Rohden, A. Sorge, D. Witthaut, M. Timme, Chaos: An Interdisciplinary J. Nonlinear Sci. **24**(1), 013123 (2014)